Preprints of the 18th IFAC World Congress
Milano (Italy) August 28 - September 2, 2011

Linear and Nonlinear Decoupling for Inner Loop Power Control in 3G Mobile Communications

K. Lau, G. C. Goodwin, M. Cea * and T. Wigren **

* *ARC Centre for Dynamic Systems and Control*
The University of Newcastle
Callaghan, NSW 2308, AUSTRALIA.
{K.Lau, Graham.Goodwin}@newcastle.edu.au,
mauricio.cea@uon.edu.au
** *WCDMA System Management*
Ericsson AB
SE-164 80 Stockholm, SWEDEN
torbjorn.wigren@ericsson.com

Abstract: Inner loop power control is a crucial part of the operation of 3G mobile communication systems. This is necessary to deal with the, so called, 'near-far' problem and to combat the effects of time variations in the channel gain. In practice, power control is dealt with in a decentralized fashion, i.e., using one SISO control loop for each user. However, significant multivariable coupling occurs due to the fact that each user is a source of interference to every other user. This means that the actual performance is significantly degraded relative to the idealized SISO case. In this paper, we describe a novel nonlinear decoupling algorithm for the uplink of the WCDMA 3G cellular system which effectively compensates for the MIMO interactions. We also develop a simplified linearized form of the algorithm. We explore the relative merits of the scheme for typical mobile communication scenarios incorporating grant changes, fading and quantization. Our simulations show that, in all cases, the decoupling strategies lead to significant performance gains relative to the use of decentralized strategies in common use.

1. INTRODUCTION

Power control is necessary for the successful operation of third generation (3G) communication systems. In particular, power control is needed to compensate for time variations in the channel gains (known as fading) and to address the 'near-far' effect, whereby a user who is close to a base station overpowers one who is further away. The power control algorithms in 3G systems are generally SIR (signal-to-interference-ratio) based (i.e., they control the SIR for each user). The resulting control problem is inherently multivariable, since each user is a source of interference to every other user.

The problem of power control for wireless networks has been studied in some detail in the communication and control literature. A detailed survey of results in this field is provided in Koskie and Gajic [2006], whilst an overview may be found in Rintamäki [2002]. The problem is analyzed in a control theory framework in Gunnarsson and Gustafsson [2003], and an overview of the limitations of power control in wideband code division multiple access (WCDMA) 3G systems is given in Gunnarsson [2001].

Centralized algorithms, such as the one described in Zander [1992a], calculate the required powers (or control actions) for all of the users. These algorithms typically assume full knowledge of the link gains at all controller nodes. Hence they are not usually implemented due to the high signalling overhead required. In practice, distributed algorithms (e.g.,Zander [1992b] and Foschini and Miljanic [1993]) are often used. These require only local measurements (i.e., the SIR at each receiver) to adjust the power of each user in a decentralized manner.

Modern 3G systems, including WCDMA systems, typically employ SISO control loops to compensate for time variations in the channel gains and interference levels. On the uplink of 3G systems, a cascade scheme, consisting of a fast inner loop and a slow outer loop, is often used. The role of the inner power control loop is to maintain the signal-to-interference ratio (SIR) for each user at an approximately constant (target) level. The target SIR is adjusted by the slow outer loop to maintain a constant block error rate.

The design of SISO inner power control loops has been studied in a number of papers including Gunnarsson et al. [2001], Rintamäki et al. [2004] and Agüero et al. [2009]. In the present paper, we propose a novel nonlinear decoupling scheme for inner loop power control on the uplink of WCDMA systems. The scheme compensates for the multivariable coupling which is inherent to SIR control. Whilst the scheme is a centralized scheme, we note that only local SIR measurements (i.e., at the base station) are required. We also develop a simplified linearized form

⋆ This work was supported by an Australian Research Council Linkage Grant and by Ericsson AB, Sweden.

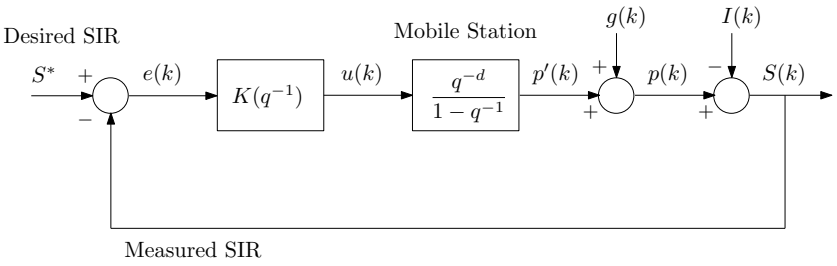

Fig. 1. SISO inner power control loop.

of the algorithm. The effect of grant changes, quantization, and fading will be considered.

The layout of the remainder of the paper is as follows: In Section 2, a detailed description of the system is given. Then, in Section 3, we describe the SISO controller which is used to demonstrate the decoupled schemes. The nonlinear and linear schemes are derived in Sections 4 and 5, respectively. The effects of channel gain variations and quantization are briefly discussed in Section 6. Conclusions are given in Section 7.

2. SYSTEM DESCRIPTION

As mentioned in the introduction, WCDMA (3G) systems typically employ SISO power control loops. A simplified block diagram of the (uplink) inner power control loop for a single mobile user is shown in Fig. 1. In this figure, all of the quantities are expressed in logarithmic scale (dB). Note that, here and in the sequel, quantities may be expressed in either linear or logarithmic scales. A bar$^-$ is used to denote a linear quantity.

The control loop operates as follows: The mobile station continuously transmits a signal on the dedicated physical control channel (DPCCH) in the uplink using a transmission power of $p'(k)$. The transmission power is controlled by the base station, which sends power commands (in the form of power increments in dB) to the user at each time k.

In Fig. 1, $p'(k)$ is the transmitted power at time k and $p(k)$ is the received signal power. The disturbances $g(k)$ and $I(k)$ are the time varying channel (fading) gain and the interference power, respectively. We note that the channel gain and interference become additive disturbances in the logarithmic scale. The output $S(k)$ is the measured SIR at the receiver, and the input S^* is the target SIR (assumed to be constant). The error $e(k) = S^* - S(k)$ is fed into the controller $K(q^{-1})$ to calculate the power increment $u(k)$. The mobile station is modelled as an integrator and a time delay d. This corresponds to the loop delay and is assumed to be constant and known. The sampling period used in WCDMA systems is 667 μs.

The DPCCH signal is transmitted from the mobile station to the base station for the purpose of power control. The user also transmits data simultaneously using a power of $\bar{\gamma}(k)\bar{p}'(k)$. In the case of enhanced uplink (EUL) traffic [Dahlman et al., 2007], the scaling factor $\bar{\gamma}(k)$ is referred to as the power grant. EUL consists of control and data components which are sent on different WCDMA channels, namely, the enhanced dedicated physical control channel (E-DPCCH) and the enhanced dedicated physical data channel (E-DPDCH), respectively. These signals occupy the same frequency band but are separated by codes that are not perfectly orthogonal in the uplink. It is assumed that the DPCCH and EUL signals experience similar channel conditions, and hence that the received power and SIR for the EUL signal are given by $\bar{\gamma}(k)\bar{p}(k)$ and $\bar{\gamma}(k)\bar{S}(k)$, respectively. This implies that the grant determines the nominal SIR of the EUL signal, and hence, the grant is closely related to the achievable data rate. The power grants are scheduled by the base station, which attempts to co-ordinate data transmissions from the users whilst keeping the total interference at an acceptable level. A more detailed explanation of the operation of the uplink can be found in Chapter 10 of Dahlman et al. [2007].

We now discuss the multivariable interactions which arise when there is more than one user. Let n be the total number of users, and let quantities related to the ith user be denoted by a subscript i. The SIR for user i is given by

$$\bar{S}_i(k) = \frac{\bar{p}_i(k)}{\bar{I}_i(k)}, \tag{1}$$

where

$$\bar{I}_i(k) = \sum_{\substack{j=1,\\ j\neq i}}^{n} (1+\bar{\gamma}_j(k))\bar{p}_j(k) + \bar{\alpha}(1+\bar{\gamma}_i(k))\bar{p}_i(k) + \bar{N}_0. \tag{2}$$

In this expression, $(1+\bar{\gamma}_j(k))\bar{p}_j(k)$ is the interference due to user j, $\bar{\alpha}(1+\bar{\gamma}_i(k))\bar{p}_i(k)$ is the 'self-interference' (also known as 'auto-interference'), and $\bar{N}_0$ consists of thermal noise and other sources of interference (including inter-cell interference). In this paper, we assume that $\bar{N}_0$ is constant. The self-interference term in (2) is used to account for the fact that only a fraction of the received power is 'useful' [Godlewski and Nuaymi, 1999]. The rest acts as interference. From equations (1) and (2), it is clear that the SIRs for the users are coupled in a nonlinear manner.

Note that we assume that the target SIR S^* is *feasible*. By this we mean that there exist $\bar{p}_i^* > 0$ such that $\bar{p}_i = \bar{p}_i^*$ satisfies

$$S_i = S^*$$

for all i ([Gunnarsson and Gustafsson, 2003]). The coupling between the users implies that if the power grant for one user is changed, then the target power levels p_i^* for all of the users will change.

We initially ignore quantization. However, in practice, this has a profound effect on the performance of the inner power control loop. We will show later in the paper that quantization effects can be mitigated by the use of adaptive quantization schemes. Indeed, with these schemes

the achieved performance with and without quantization are comparable.

3. SISO CONTROLLER DESIGN

In this section, we describe a SISO controller $K(q^{-1})$ for inner loop power control. The controller will be used to demonstrate the decoupling algorithms presented later in the paper, and is given by

$$K(q^{-1}) = \frac{1}{1 + q^{-1} + ... + q^{-d+1}}. \tag{3}$$

The transfer function above has been considered previously [Gunnarsson et al., 2001, Agüero et al., 2009], and can be derived in variety of ways. For example, it can be shown that, if $g(k) - I(k)$ is modelled as a random walk, then $K(q^{-1})$ is the minimum variance controller. This is stated formally in the following theorem:

Theorem 1. Consider the closed loop system in Fig. 1. Suppose that $g(k) - I(k)$ can be modelled as

$$\frac{q^{-1}}{1 - q^{-1}} w(k),$$

where $w(k)$ is a white noise sequence. Then the controller given by (3) minimizes the variance of $S(k)$ due to $g(k) - I(k)$.

Proof. The result follows from [Agüero et al., 2009, Theorem 1]. □

Alternatively, the controller can be viewed as a time delay compensator. This is the approach taken in Gunnarsson et al. [2001].

Further insight can be gained by considering the case of a single user with $\bar{\alpha} = 0$ and $g(k) = 0$. In this case, $I(k)$ is independent of $p(k)$ and the closed loop transfer function from $I(k)$ to $p(k)$ is given by q^{-d}. It follows that

$$p(k) = S^* + I(k - d)$$

and

$$S(k) = S^* + I(k - d) - I(k).$$

This implies that if $I(k)$ is a step disturbance, then the SIR will return to its target value after d samples.

We now consider the case of two users with $\bar{I}_i(k)$ given by (2). Fig. 2 shows the simulated responses with $\bar{S}^* = 1/64$, $g(k) = 0$, $\bar{\alpha} = 0.3$, $d = 2$ and $\bar{N}_0 = 3 \times 10^{-11}$ mW. Each user is controlled using a SISO loop of the form shown in Fig. 1 with $K(q^{-1})$ given by (3). For this simulation, $\bar{\gamma}_1(k) = 8$ and $\bar{\gamma}_2(k)$ is changed from 70 to 100 at $k = 15$ ($t = 10$ ms). The dashed lines indicate the equilibrium (target) power levels which correspond to the specified power grants.

From Fig. 2, it can be seen that the SIR and power responses converge relatively slowly to their equilibrium values after the change in the power grant for user 2. This is due to the coupling between the power control loops and the effect of self-interference.

4. NONLINEAR DECOUPLING SCHEME

We propose a decoupling scheme which is based on the nonlinear function which relates the SIRs of the users to their received powers.

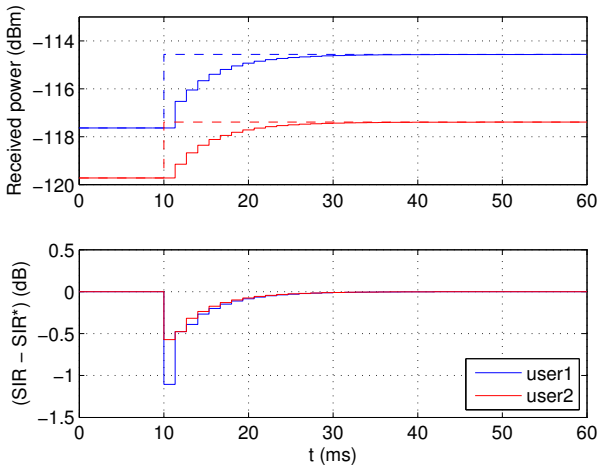

Fig. 2. Closed loop responses for two users with no decoupling.

In the discussion that follows, boldface is used to denote the vector equivalent of the corresponding scalar quantity. Hence $\mathbf{p} = [p_1 \;\; p_2 \;\; ... \;\; p_n]^T$, $\bar{\mathbf{I}} = [\bar{I}_1 \;\; \bar{I}_2 \;\; ... \;\; \bar{I}_n]^T$, etc.

We first observe that $\mathbf{S}$ is given by $\mathbf{f}_\gamma(\mathbf{p})$, where $\mathbf{f}_\gamma$ is the nonlinear vector function defined by the following sequence of equations:

$$\bar{p}_i = 10^{0.1 p_i}, \tag{4}$$

$$\bar{\mathbf{I}} = \mathbf{A}\bar{\mathbf{p}} + \mathbf{b}, \tag{5}$$

$$I_i = 10 \log_{10} \bar{I}_i, \tag{6}$$

$$\mathbf{f}_\gamma(\mathbf{p}) = \mathbf{p} - \mathbf{I}. \tag{7}$$

In equation (5), the matrix $\mathbf{A}$ and vector $\mathbf{b}$ can be found by rewriting (2) in vector form. For the case of two users, we obtain

$$\mathbf{A} = \begin{bmatrix} \bar{\alpha}(1 + \bar{\gamma}_1) & (1 + \bar{\gamma}_2) \\ (1 + \bar{\gamma}_1) & \bar{\alpha}(1 + \bar{\gamma}_2) \end{bmatrix} \quad \text{and} \quad \mathbf{b} = \begin{bmatrix} \bar{N}_0 \\ \bar{N}_0 \end{bmatrix}.$$

With the above definitions, we see that the MIMO system from $\mathbf{u}$ to $\mathbf{S}$ can be modelled as shown in Fig. 3. In this figure, $\mathbf{D}$ is the $n \times n$ identity matrix.

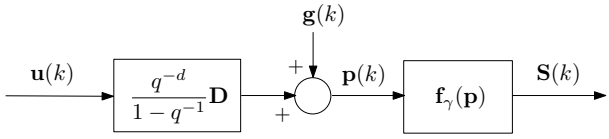

Fig. 3. MIMO model of the system from $\mathbf{u}$ to $\mathbf{S}$.

We assume that $\mathbf{f}_\gamma$ represents a 'true' model of the coupling between the users. In practice, only an approximate model, in which some of the true parameters are replaced by estimates, will be available. In particular, we note that the quantity $\bar{N}_0$ needs to be estimated. This is because $\bar{N}_0$ is defined at the antenna connector. However, it is measured in the digital receiver after passing cabling and front-end electronics. This introduces scale factor errors of the order of 1 dB. The estimation of $\bar{N}_0$ is non-trivial during operation since neighbor cell interference affects the uplink power. Techniques for such estimation are, for example, described in Wigren [2010]. We let $\hat{\mathbf{f}}_\gamma$ be the

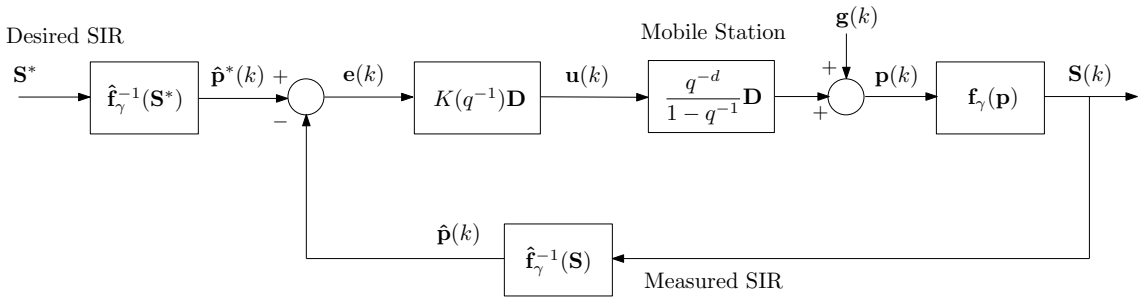

Fig. 4. Nonlinear decoupling scheme.

estimated coupling model, and let $\hat{\mathbf{b}}$ denote the estimate for $\mathbf{b}$.

We have shown that the coupling between the users is fully described by a nonlinear function. This suggests that we use the inverse of the (estimated) function for decoupling. Let $\bar{\mathbf{S}}_\mathbf{D}$ be the diagonal matrix given by

$$\bar{\mathbf{S}}_\mathbf{D} = \mathrm{diag}(\bar{\mathbf{S}}) = \begin{bmatrix} \bar{S}_1 & 0 & \dots & 0 \\ 0 & \bar{S}_2 & \dots & 0 \\ \vdots & \vdots & \ddots & \vdots \\ 0 & 0 & \dots & \bar{S}_n \end{bmatrix}.$$

It can be easily verified that $\hat{\mathbf{f}}_\gamma^{-1}$ is defined by the following sequence of equations:

$$\bar{S}_i = 10^{0.1 S_i}, \tag{8}$$

$$\hat{\bar{\mathbf{p}}} = \left(\mathbf{D} - \bar{\mathbf{S}}_\mathbf{D}\mathbf{A}\right)^{-1} \bar{\mathbf{S}}_\mathbf{D}\hat{\mathbf{b}}, \tag{9}$$

$$\hat{p}_i = 10 \log_{10} \hat{\bar{p}}_i \tag{10}$$

$$\hat{\mathbf{f}}_\gamma^{-1}(\mathbf{S}) = \hat{\mathbf{p}}. \tag{11}$$

We assume that the matrix inverse in Equation (9) exists.

Fig. 4 shows a nonlinear decoupling scheme which utilizes $\hat{\mathbf{f}}_\gamma^{-1}$. In this scheme, $\mathbf{S}(k)$ is passed through $\hat{\mathbf{f}}_\gamma^{-1}$ to generate an estimate of the power vector $\hat{\mathbf{p}}(k)$. In the ideal case (in which $\mathbf{f}_\gamma = \hat{\mathbf{f}}_\gamma$), the resulting open loop system from $\mathbf{u}(k)$ to $\hat{\mathbf{p}}(k)$ is perfectly decoupled. Since the output of the new open loop system is $\hat{\mathbf{p}}(k)$, we also convert $\mathbf{S}^*$ to an equivalent target for $\hat{\mathbf{p}}$. This is achieved by passing $\mathbf{S}^*$ through $\hat{\mathbf{f}}_\gamma^{-1}$ to generate $\hat{\mathbf{p}}^*(k)$. The error between $\hat{\mathbf{p}}^*(k)$ and $\hat{\mathbf{p}}(k)$ is fed back through a diagonal controller to calculate $\mathbf{u}(k)$.

It may be observed that, for the scheme shown in Fig. 4, $\mathbf{e}(k) = 0$ implies that $\mathbf{S}(k) = \mathbf{S}^*$. This is due to the fact that $\hat{\mathbf{p}}(k)$ and $\hat{\mathbf{p}}^*(k)$ are generated using the same nonlinear function. However, it should also be noted that if $\hat{\mathbf{p}}(k)$ is replaced by an alternative estimate of the power vector, then the observation made above may no longer hold.

Fig. 5 shows the nominal (ideal) closed loop responses for the case of two users. The parameters used for the simulation are the same as those used in Section 3. It can be seen that the responses resemble the response for a single user described in Section 3. In particular, the system settles to its new equilibrium point exactly d samples ($d = 2$ in this case) after the power grant change. This is due to the fact that, in the ideal case, $\hat{\mathbf{p}}(k) = \mathbf{p}(k)$ is independent of the choice of the grants $\bar{\gamma}_i(k)$. Hence, changing a power grant is equivalent to changing $\hat{\mathbf{p}}^*(k)$.

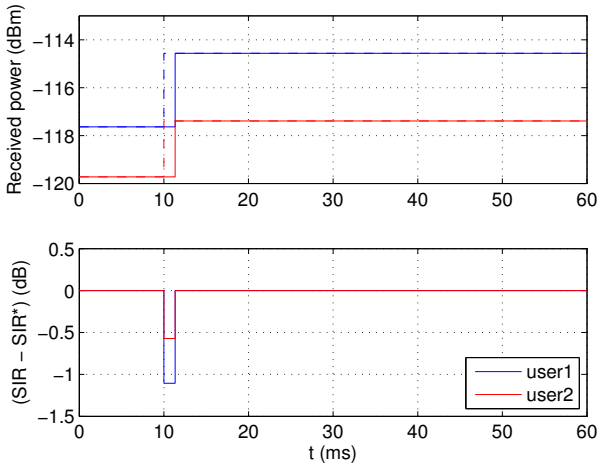

Fig. 5. Closed loop responses for two users with nonlinear decoupling.

5. LINEAR DECOUPLING SCHEME

In this section, we develop a simplified linear version of the nonlinear decoupling scheme from the previous section.

By taking a first order Taylor approximation, we can obtain the following linearized model of the coupling:

$$\mathbf{S} \approx \mathbf{S}^* + \hat{\mathbf{M}}_\gamma(\mathbf{p} - \hat{\mathbf{p}}^*),$$

where $\hat{\mathbf{M}}_\gamma = [m_{ij}]$ and

$$m_{ij} = \left.\frac{\partial \hat{f}_i}{\partial p_j}\right|_{\hat{\mathbf{p}}^*}.$$

In the above expression, $\hat{f}_i$ is the ith component the estimated coupling model $\hat{\mathbf{f}}_\gamma$, and $\hat{\mathbf{p}}^*$ is the target power vector (defined previously).

By differentiating $\hat{\mathbf{f}}_\gamma$ and evaluating the resulting expression at $\hat{\mathbf{p}}^*$, it can be shown that

$$\hat{\mathbf{M}}_\gamma = \mathbf{D} - \bar{\mathbf{S}}_\mathbf{D}\mathbf{P}_\mathbf{D}^{-1}\mathbf{A}\mathbf{P}_\mathbf{D},$$

where $\mathbf{P}_\mathbf{D} = \mathrm{diag}(\hat{\mathbf{p}}^*)$.

For the case of two users, $\hat{\mathbf{M}}_\gamma$ is given by

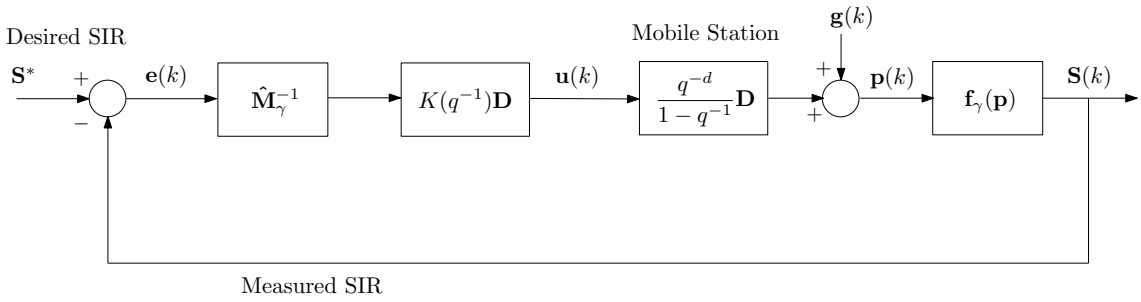

Fig. 6. Linear decoupling scheme.

$$\hat{\mathbf{M}}_\gamma = \begin{bmatrix} 1-\bar{\alpha}(1+\bar{\gamma}_1)\bar{S}^* & -(1+\bar{\gamma}_2)\bar{S}^*\dfrac{\hat{\bar{p}}_2^*}{\hat{\bar{p}}_1^*} \\ -(1+\bar{\gamma}_1)\bar{S}^*\dfrac{\hat{\bar{p}}_1^*}{\hat{\bar{p}}_2^*} & 1-\bar{\alpha}(1+\bar{\gamma}_2)\bar{S}^* \end{bmatrix}.$$

Since $\mathbf{e} = \mathbf{S} - \mathbf{S}^*$, the matrix $\hat{\mathbf{M}}_\gamma$ describes the coupling between the individual SIR errors. It follows that $\hat{\mathbf{M}}_\gamma^{-1}$ can be used to decouple the errors. The resulting scheme is shown in Fig. 6.

Simulated responses for the linear decoupling scheme with two users are shown in Fig. 7. It can be seen that the responses are almost as good as those shown in Fig. 5 for the nonlinear scheme.

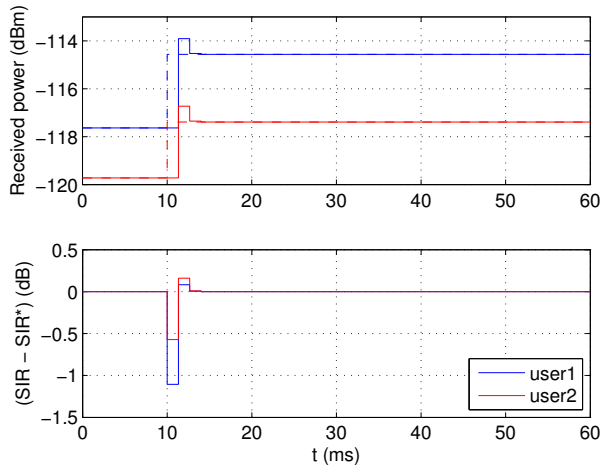

Fig. 7. Closed loop responses for two users with linear decoupling.

6. EFFECT OF GAIN VARIATIONS AND QUANTIZATION

For the main part of this paper, we have ignored the effect of channel gain variations and quantization. In this section, we briefly discuss the effect of channel gain variations and quantization on the performance of the proposed decoupling schemes.

In order to illustrate the effect of channel gain variations, we repeat the simulations corresponding to Fig. 2 (no decoupling) and Fig. 7 (linear decoupling) with $g_i(k)$ given by simulated Rayleigh fading. A two-step-ahead predictor is used to compensate for the channel variations. Figs. 8 and 9 show the results of the simulations. The channel gains $g_1(k)$ and $g_2(k)$ which are used in the simulations are shown in Fig. 10. It can be seen that the decoupled scheme still performs well, and the simulated power responses appear to be slightly better than those for the coupled case.

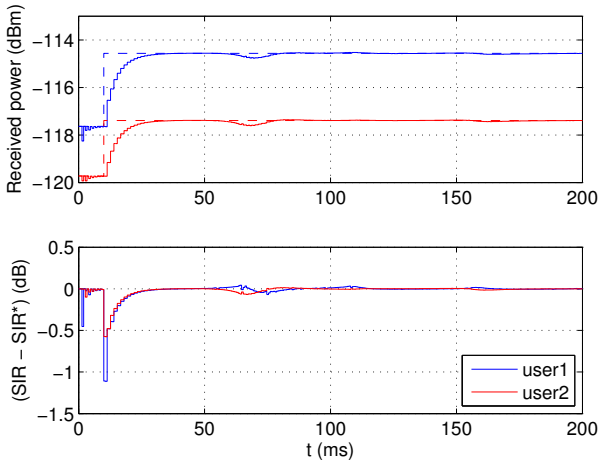

Fig. 8. Closed loop responses with time-varying channel gains and no decoupling.

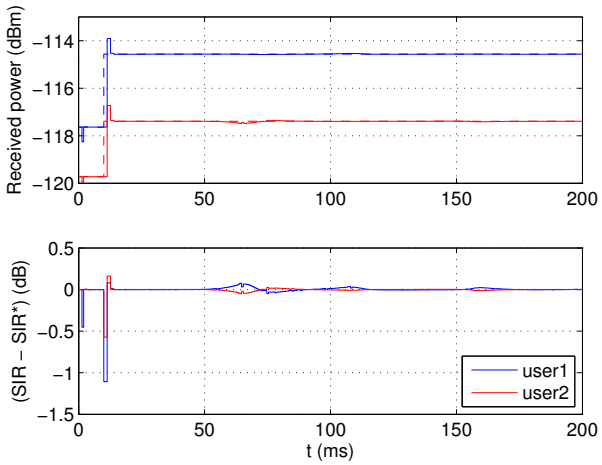

Fig. 9. Closed loop responses with time-varying channel gains and linear decoupling.

Quantization of the control signal is also a significant problem for inner loop power control. In practice, the control signal is often transmitted using only one bit. If

a standard one-bit quantizer is used, then most of the improvement due to decoupling will be lost. However, if adaptive quantization is used, then most of the benefits of decoupling may be retained. We demonstrate this using an adaptive quantizer which is similar, but not identical, to those described in Al Mamun et al. [2009] and Khan and Jain [2009]. The simulated responses with linear decoupling are shown in Fig. 11. Comparing the responses to those in Figs. 2 and 7, we see that the quantized responses are slightly worse than the responses with linear decoupling, but significantly better than those without any decoupling.

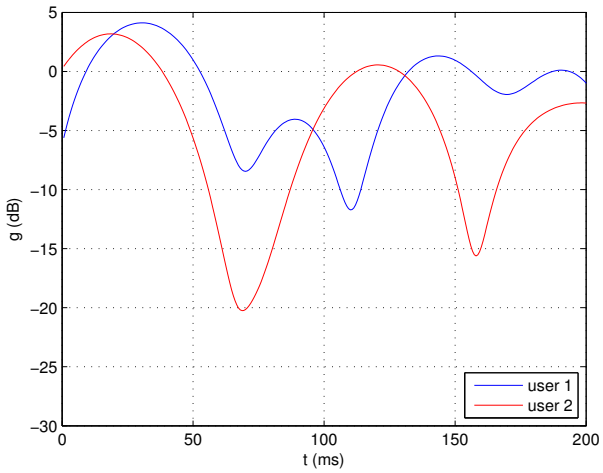

Fig. 10. Channel gain variations used for the simulation results in Figs. 8 and 9.

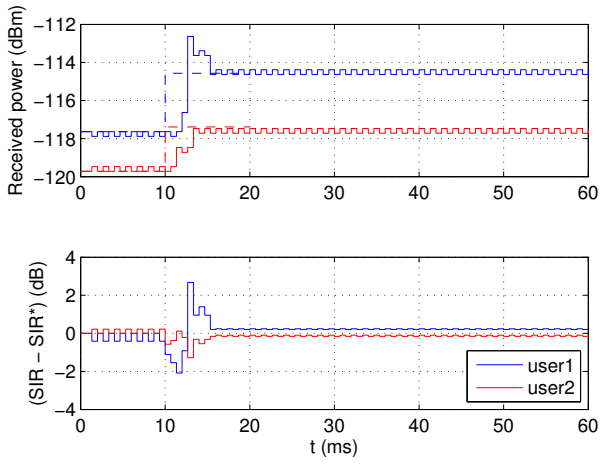

Fig. 11. Closed loop responses with an adaptive one-bit quantizer and linear decoupling.

7. CONCLUSION

This paper has discussed both nonlinear and linear decoupling schemes for inner loop power control on the uplink of 3G communications systems. Simulations have verified that the proposed schemes lead to significant improvements in transient performance relative to the decentralized scheme in common use.

REFERENCES

J. C. Agüero, G. C. Goodwin, K. Lau, M. Wang, E. I. Silva, and T. Wigren. Three-degree of freedom adaptive power control for CDMA cellular systems. In *Proc. of the IEEE Global Communications Conference (Globecom 2009)*, Hawaii, USA, 2009.

A. Al Mamun, S. Islam, F. Yesmin, M. Akter, and S. A. Jahan. Novel adaptive step power control algorithm for 3G WCDMA cellular system. In *Proc. of the 12th International Conference on Computers and Information Technology (ICCIT '09)*, pages 526–530, 2009.

E. Dahlman, S. Parkvall, J. Sköld, and P. Beming. *3G Evolution: HSPA and LTE for Mobile Broadband*. Academic Press, 2007.

G. J. Foschini and Z. Miljanic. A simple distributed autonomous power control algorithm and its convergence. *IEEE Transactions On Vehicular Technology*, 42 (4):641–646, Nov. 1993.

P. Godlewski and L. Nuaymi. Auto-interference analysis in cellular systems. In *Proc. of the 49th IEEE Vehicular Technology Conference*, pages 1994–1998, 1999.

F. Gunnarsson. Fundamental limitations of power control in WCDMA. In *Proc. of the 54th IEEE Vehicular Technology Conference*, pages 630–634, 2001.

F. Gunnarsson and F. Gustafsson. Control theory aspects of power control in UMTS. *Control Engineering Practice*, 11(10):1113–1125, Oct. 2003.

F. Gunnarsson, F. Gustafsson, and J. Blom. Dynamical effects of time delays and time delay compensation in power controlled DS-CDMA. *IEEE Journal On Selected Areas In Communications*, 19(1):141–151, Jan. 2001.

M. A. R. Khan and P. C. Jain. A simple modified fixed step size power control algorithm for CDMA cellular systems. In *Proc. of the International Conference on Multimedia, Signal Processing and Communication Technologies (IMPACT '09)*, pages 134–137, 2009.

S. Koskie and Z. Gajic. Signal-to-interference-based power control for wireless networks: A survey, 1992–2005. *Dynamics of Continuous, Discrete and Impulsive Systems B: Applications and Algorithms*, 13(2):187–220, 2006.

M. Rintamäki. *Power control in CDMA cellular communication systems*. Wiley Encyclopedia of Telecommunications, Vol. IV. Wiley, 2002.

M. Rintamäki, H. Koivo, and I. Hartimo. Adaptive closed-loop power control algorithms for CDMA cellular communication systems. *IEEE Transactions On Vehicular Technology*, 53(6):1756–1768, Nov. 2004.

T. Wigren. Recursive noise floor estimation in WCDMA. *IEEE Transactions On Vehicular Technology*, 59(5): 2615–2620, June 2010.

J. Zander. Performance of optimum transmitter power control in cellular radio systems. *IEEE Transactions On Vehicular Technology*, 41(1):57–62, Feb. 1992a.

J. Zander. Distributed cochannel interference control in cellular radio systems. *IEEE Transactions On Vehicular Technology*, 41(3):305–311, Aug. 1992b.